The shock compression of microorganism-loaded broths and emulsions: Experiments and simulations

P.J. Hazell, C. Beveridge, K. Groves, G. Appleby-Thomas

Accepted Manuscript

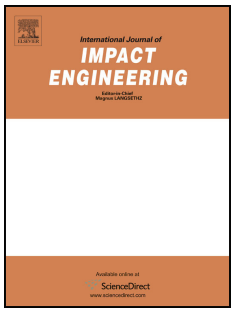

Title: The shock compression of microorganism-loaded broths and emulsions: Experiments and simulations

Authors: P.J. Hazell, C. Beveridge, K. Groves, G. Appleby-Thomas

PII: S0734-743X(09)00160-2

DOI: 10.1016/j.ijimpeng.2009.08.007

Reference: IE 1827

To appear in: *International Journal of Impact Engineering*

Received Date: 27 March 2009

Revised Date: 21 August 2009

Accepted Date: 24 August 2009

Please cite this article as: Hazell PJ, Beveridge C, Groves K, Appleby-Thomas G. The shock compression of microorganism-loaded broths and emulsions: Experiments and simulations, International Journal of Impact Engineering (2009), doi: 10.1016/j.ijimpeng.2009.08.007

The shock compression of microorganism-loaded broths and emulsions: experiments and simulations

P J Hazell[1], C Beveridge[2,3],K Groves[2] and G Appleby-Thomas[1]

[1]Cranfield Defence and Security, Cranfield University, Shrivenham, Swindon, SN6 8LA

[2]Leatherhead Foods International, Randalls Road, Leatherhead, Surrey, KT22 7RY

[3]Present address: CBC, 49 Adkin Way, Wantage, Oxfordshire, OX12 9HN

ABSTRACT

By carefully selecting flyer plate thickness and the geometry of a target capsule for bacterial broths and emulsions, we have successfully subjected the contents of the capsule to simultaneous shock and dynamic compression when subjected to a flyer-plate impact experiment. The capsules were designed to be recovered intact so that post experimental analysis could be done on the contents. ANSYS® AUTODYN hydrocode simulations were carried out to interrogate the deformation of the cover plate and the wave propagation in the fluid. Accordingly, we have shown that microorganisms such as *Escherichia coli, Enterococcus faecalis* and *Zygosaccharomyces bailii* are not affected by this type of loading regime. However, by introducing a cavity behind the broth we were able to observe limited kill in the yeast sample. Further, on using this latter technique with emulsions it was shown that greater emulsification of an oil-based emulsion occurred due to the cavitation that was introduced.

Keywords: shock wave; capsule design; bacteria; yeast; emulsification

[1]Tel: +44 (0) 1793 785731; Email: p.j.hazell@cranfield.ac.uk

INTRODUCTION

The shock behaviour of fluids has been extensively studied over the years using flyer-plate techniques. This is a standard approach that invokes a condition of uniaxial strain in both the target and the flyer plate leading to the formation of a shock wave in both. Typically the fluid is contained in a capsule that is usually destroyed on impact, during which the particle velocity is measured either by using a VISAR (Velocity Interferometer System for Any Reflector) system or inferred from the time-of-arrival of the shock measured by two spatially separated gauges, the Hugoniot properties of the flyer plate and its impact velocity.

The behaviour of bacterial broths that have been subjected to shock loading has also been the subject of a number of studies. Usually, this is achieved either by electrohydraulic action where an electrodischarge generates a shock wave in a suspension e.g., [1] or by using an explosive charge [2,3] where pressures of several hundreds of MPa are expected. Some studies have also focussed on high velocity plate impact studies where gas-driven or explosively-driven flyer plates are accelerated to high velocities. The impact of these flyer plates has resulted in high shock pressures (many GPa scale) being generated in spore-loaded minerals such as gabbro [4]. Other researchers have used high pressure shock tubes for dynamically loading the biological sample [5] whereas other experiments have centred around hypervelocity impacts where spherical projectiles are accelerated to hypervelocity (c.a. 2-5 km/s) which results in large shock pressures (many GPa scale) being temporarily sustained by the organisms in question [6].

The behaviour of bacterial spores being subjected to shock wave loading is important, not least as it could provide an alternative route to pasteurisation. Loske et

al. [7] subjected *E. coli* in suspension to hundreds of shock waves using an electrohydraulic shock wave generator. Using a parabolic reflector, they showed it was possible to produce a plane shock front and expose many samples to shock at the same time. Experimental results indicated that electrohydraulically generated shock waves are capable of producing a significant reduction in an *E. coli* population with average shock magnitudes of 44 MPa. However, the authors also pointed out that their system generated UV light that could have contributed to the kill mechanism. Furthermore, a negative pressure pulse of 6 MPa was also measured which ultimately would have caused cavitation, again possibly contributing to the kill mechanism. Zuckerman et al. [8] generated pressures ranging from 80 to 100 MPa using a piezoelectric probe. They showed that up to 7.5 log reduction was observed for *E. coli* after the application of five pulses. Furthermore, a 4-5 log reduction of Lactic acid and *Staphlococcus aureus* was also seen when subjected to identical loading conditions to the *E. coli*. Again, it was thought that UV radiation may have played a part in the lethal effects.

There is evidence that certain types of bacteria are made inactive when subjected to certain pressure regimes. Abe et al. [9] loaded a bacterial broth housed in an aluminium capsule such that pressures of 200 MPa resulted in the inactivation of marine *Vibrio* sp that had been isolated from sea water. Electron microscope and protein analysis showed that the shock waves did not kill the bacteria; instead the bacteria were deformed by the process. Whereas, shock pressures generated by shock wave lithotripsy in a vat of water containing *E. coli* and *Listeria monocytogenes* resulted in no inactivation with up to 8000 single shock waves of magnitude 38 MPa [10]. Nevertheless there was a reduction in activity when multiple dual shock waves were used.

There is however, some evidence that yeast has increased mortality under high shock pressure. Kani [11] used a powder gun to accelerate copper flyer discs at a stainless steel capsule containing yeast. In this work the author showed that applying a shock pressure of c.a. 1 GPa, provided by an impact velocity of 450 m/s, the vital force became weak (assessed by the reduction in cultivated colonies after shock loading); it was suggested that it may even disappear altogether with an increase in applied pressure.

There is some evidence that certain bacteria survive very high shock pressures. For example, Burchell et al. [12] has shown that when transient shock pressures are formed from hypervelocity impacts of spherical projectiles into targets, *Rhodococcus erythropolis* cells survive. The authors noted that although survival rates were low at a shock pressure of 78 GPa, they were still finite. Their results indicated that survival fell with a log law as the shock pressure increased. They also noted that for a different organism, *Bacillis subtilis*, the survival rate at 78 GPa was found to be higher than that of the *Rhodococcus erythropolis* indicating that survival rate may well depend on the type of bacteria. Stöffler et al. [4] has also shown high survival rates of bacterial spores (*Bacillus subtilis*), cyanobacteria (*Chroococcidiopsis sp.*), and lichen (*Xanthoria elegans*) embedded in gabbro when subjected to high shock stresses (>10 GPa). Willis et al. [13] also reported limited mortality rates for *Escherichia coli* shocked to an initial shock pressure of 0.26 GPa using the flyer-plate technique. Unlike most other previous work, they were able to shock their bacteria in suspension to high pressures. However, they were only able to recover one of the four samples in the original liquid with the other three requiring re-suspension. As the authors point out this may have affected the recorded survival rates for 3 of the 4 samples. Where

dead bacteria were recovered, they were able to conduct TEM analysis that revealed cell wall rupture and delamination.

Some of these experimental techniques are disadvantaged in that they produce simultaneous cavitation in the medium as well as high shock pressure, they generate UV light or they do not allow for sample recovery after the experiment without risk of contamination. Cavitation is also a concern as this is also thought to contribute to the kill mechanism of bacteria. In this paper, we report the design of a capsule that can be used during 1D uniaxial strain plate impact experiments to shock compress a volume of fluid to c.a. 1.2 GPa where cavitation is suppressed by virtue of the dynamic loading by a front plate. Additionally, modification to the design of the capsule to allow the introduction of controlled levels of cavitation in the sample is discussed. The capsule was designed to be recoverable so that no contamination would occur during the experiment. ANSYS® AUTODYN hydrocode simulations are also presented that show the ringing up of the shock within the fluid layer as well as the pressures achieved in dynamic (cover-plate) compression. Results are presented that show that *Escherichia coli*, *Enterococcus feacalis* and *Zygosaccharomyces bailii* are not affected by high compressive loads where cavitation is suppressed which suggests that the main mechanisms of kill seen by previous researchers using pulsed electrical discharges was not due to the shock pressure. Finally, by testing coarse emulsions using the same technique we will show that it is possible to induce cavitation leading to significant emulsification of the sample.

EXPERIMENTAL DESIGN

Background to the experiment

Plate impact experiments are commonly used to induce shock waves in target materials. In the plate impact configuration, targets are struck with flying-plates carefully aligned so that all points on the projectile's surface make contact with the target simultaneously. This requires that both the impacting plate and the target are flat and parallel to within a tolerance of micrometres. The impact of a flyer-plate generates a planar shock wave in the target. In this situation, all strain is accommodated along the impact axis while the orthogonal components of strain are zero due to inertial confinement. Consequently, the orthogonal components of stress are non-zero. Therefore in summary, the conditions of stress and strain in the target are:

$$\varepsilon_x \neq \varepsilon_y = \varepsilon_z = 0 \text{ and } \sigma_x \neq \sigma_y = \sigma_z \neq 0,$$

where subscript *x* is denotes the condition along the impact axis and subscripts *y* and *z* denote the conditions orthogonal to the impact axis.

Capsule design

The capsule was manufactured from AISI 304 L by RTS (Leeds) Ltd. The manufacturer's data sheet stated a UTS value of 591 MPa and an elongation to failure of 55%. The elastic properties of the steel, as measured using 5MHz quartz

transducers with a Panametrics 5077PR pulser-receiver in the pulse-echo configuration, are shown in Table 1. The purpose of one of the experiments was to load the bacterial broths in compression to high pressures whilst at the same time suppressing cavitation in the fluid layer. To that end, ductile steel was chosen. Furthermore, this particular brand of stainless steel is commonly used within the food industry and the shock behaviour of this stainless steel is relatively well understood [14-17].

Table 1: Elastic properties of the AISI 304 L material used to manufacture the capsule.

Material	ρ_0 (g/cc)	c_L (mm/μs)	c_S (mm/μs)	G (GPa)	ν
AISI 304L	7.903	5.739	3.155	78.5	0.283

The capsule design is as shown in Figure 1. A 10-mm thick 304 L cover plate was bolted to the cup using ten M6 bolts on a 76 mm pitch-circle diameter; the diameter of the capsule was 88 mm. The test specimens were instrumented with a single manganin pressure gauge manufactured by Vishay (LM-SS-125CH-048) which was encapsulated by two 25μm Mylar layers. A copper front plate (5 mm) was used to protect the gauge. Calibration of this gauge was according to the method of Rosenberg et al. [18].

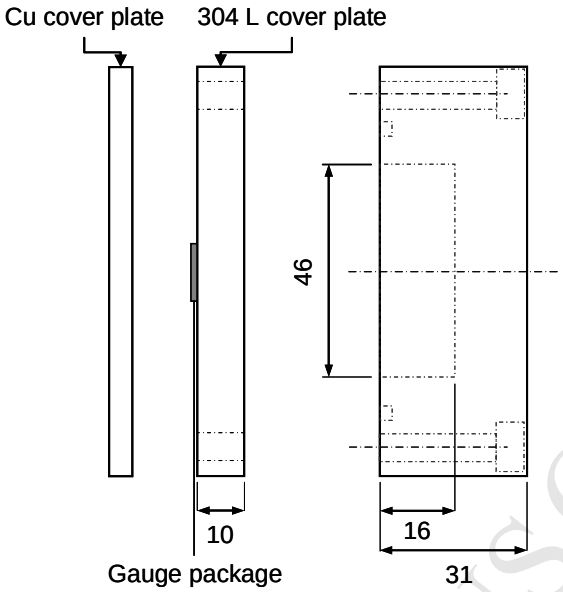

Figure 1: An exploded view of the capsule design; all dimensions are in mm.

For the first set of experiments, the capsule as shown in Figure 1 was used. In a second set of experiments, a hollow steel cylindrical insert of length 3 mm was placed in the 46-mm diameter cavity. The wall thickness of this insert was 1 mm. The purpose of the steel insert was to provide support for a 15 μm Mylar barrier that was glued to the top surface of the insert. This barrier would provide separation between the liquid sample and an air pocket trapped beneath the Mylar thereby causing cavitation in the fluid. A similar 13-mm long hollow cylinder was glued on top of the 3-mm long cylinder to sandwich the Mylar and to ensure sealing.

Experiments

All the experiments were conducted using a 50-mm single-stage light gas gun [19]. 10-mm thick copper flyer plates were accelerated to velocities of between 345

m/s and 450 m/s and were used to dynamically load each capsule containing the fluid of interest. The velocities of the projectile were measured by using a sequential pin shorting system to an accuracy of 0.5%. A fast digital storage oscilloscopes (2 GS/s) was used to capture the arrival and shape of the shock; subsequent data reduction and analysis was done on a PC. Two different types of microorganism-loaded fluids and an emulsion were tested.

Test specimens

The microorganisms used for this experiment were *Zygosaccharomyces bailii* DSM 70492 and a cocktail of *Escherichia coli* NCTC 9001 and *Enterococcus faecalis*, culture ATCC 19433. *Zygosaccharomyces bailii* is a common spoilage yeast in the food industry chiefly affecting fruit juices; *Escherichia coli* and *Enterococcus faecalis* are relatively harmless members of the normal gut flora.

The *Z. bailii* experimental culture was prepared by incubating in malt extract broth (prepared from Oxoid powder) at 25°C for 3 days to provide a 10^8 colony forming units/ml (cfu/ml). A cocktail of *E. coli* and *E. faecali*s was incubated in nutrient broth (prepared from Oxoid powder) at 37°C for 1 day to achieve the 10^8 cfu/ml. These cultures were then individually subjected to shock loading.

After subjecting the capsules to the shockwave the capsules were recovered and opened using aseptic techniques. A 1 ml sample was withdrawn and serially diluted into 8 by 9 ml of half-strength ringer's solution. 0.1 ml of each of the dilutions was then plated onto nutrient agar for incubation and subsequent numerical evaluation.

The formation of fine emulsions is an important part of food-processing industry and consequently two separate trials were carried out to evaluate the role of shock-wave application in preparation of emulsions. Coarse / crude emulsions were prepared with 10% vegetable oil, 10% gum arabic and 80% water, using a Silverson homogeniser and shock loaded in a similar fashion to that described above. The emulsions were examined by light microscopy immediately before and after firing. Analysis of the particle size distributions pre and post shock loading was performed on a Malvern Mastersizer 2000.

A summary of the experiments carried out is show in Table 2.

Table 2: Summary of flyer-plate experiments. In each case a 10-mm copper flyer-plate was used.

Sample	Flyer velocity (m/s)	Air-gap?
Bacteria	345	No
Yeast	446	No
Emulsion	345	No
Bacteria	448	Yes
Yeast	450	Yes
Emulsion	441	Yes

Numerical modelling

Hydrocode simulations were carried out to calculate the pressure in the central cavity and to confirm the dynamic (cover-plate) compression of the fluid layer, which was modelled as water. All computations were carried out using 2D axial symmetry using a Lagrangian mesh in the explicit non-linear transient dynamic numerical code – ANSYS® AUTODYN. The cell size was chosen to be 0.25 mm. This software is explained in detail elsewhere [20] and a useful overview of these types of codes is provided by Anderson [21]. However in brief, this code solves the conservations laws

of mass and momentum based on initial boundary conditions. The user is prompted for an equation of state that describes the pressure in terms of the internal energy and volume and a constitutive relationship that calculates the flow stress in terms of a number of material and application-dependent parameters including strain, strain-rate and temperature. Failure models can be introduced to describe the failure.

The equation of state for all of the materials use was of Mie-Grüneisen form [22] derived from a linear shock-particle Hugoniot thus:

$$U_s = c_0 + Su_p \tag{1}$$

where U_s and u_p are the shock and particle velocities respectively, c_0 is the bulk sound speed and S is the slope in the U_s versus u_p diagram. A Johnson-Cook strength model was applied to both the 304 L and the copper and was of the form [23]:

$$\sigma = \left(A + B{\varepsilon_p}^n\right)\left(1 + C\,ln\,\dot{\varepsilon}_p\right)\left(1 - {T_H}^m\right) \tag{2}$$

where A is the yield strength at zero plastic strain, B is the strain hardening constant, n is the strain hardening exponent, C is a strain-rate constant, T_H is the homologous temperature $(T\text{-}T_{room})/(T_m\text{-}T_{room})$ and m is the thermal softening exponent. T and T_m are the temperature and melting temperature of the material respectively.

The material models for the copper, water and epoxy resin were taken from the AUTODYN material library and are summarised in Table 2 and Table 3. Although other researchers have simulated the shock compression of water using a bi-linear Hugoniot e.g., [24], a linear Hugoniot for the water was justified given the low shock pressures that were anticipated e.g., [25]. The hydrodynamic data for the

stainless steel and the copper were taken from the AUTODYN material library whilst the Johnson-Cook strength model for the stainless steel was taken from [26]. The Johnson-Cook model for the copper is based on a slight modification to the one provided in the AUTODYN material library and was provided by [27].

Figure 2 shows the model setup. Epoxy resin was used to simulate the presence of the O-rings as both rubber and the resin have relatively low shock impedance values when compared to the stainless steel [28, 29]. Epoxy resin was also used to model the presence of the thin Mylar barrier due to its similarity in shock impedance.

Table 3: Hydrodynamic data for the copper, stainless steel, water and the epoxy resin.

	Notation	Copper	AISI 304L	H_2O	Epoxy resin
Reference density (kg/m^3)	ρ_0	8,900	7,903	1,000	1,186
Bulk sound speed (m/s)	c_0	3,958	4,570	1,483	2,730
Slope in U_s versus U_p diagram	S	1.497	1.49	1.75	1.493
Grüneisen coefficient	Γ	2.00	1.93	0.28	1.13

Table 4: Strength data for the copper and stainless steel; the Johnson-Cook data for the stainless steel was taken from [26]; the data for the copper was provided by [27]

	Notation	Copper	AISI 304L
Yield strength (MPa)	A	90	110
Work hardening constant (MPa)	B	292	1500
Work hardening exponent	n	0.05	0.36
Strain rate hardening coefficient	C	0.005	0.014
Melting temperature (°K)	T_m	1356	1696
Reference temperature (°K)	T_{room}	300	300
Thermal softening coefficient	m	1.09	1.0

The fluid layer was modelled as though it behaved in an identical fashion to water. Cavitation was assumed to occur when the pressure in the water was -10 MPa. This value is assumed to be the pressure to which the water can sustain continuous

expansion and is implemented using the P_{min} criteria within AUTODYN. This figure was based on the work of Boteler and Sutherland [30] who measured the average tensile strength for shock-induced cavitation in the water to be 8.7±0.2 MPa. In this case, when P≤-10 MPa, the pressure in the cell is set to zero until a higher (>-10 MPa) compression wave traverses the cell. This allowed visible tracking of the potential cavitation zones. An erosion strain of 200% was added to allow the simulation to progress to completeness.

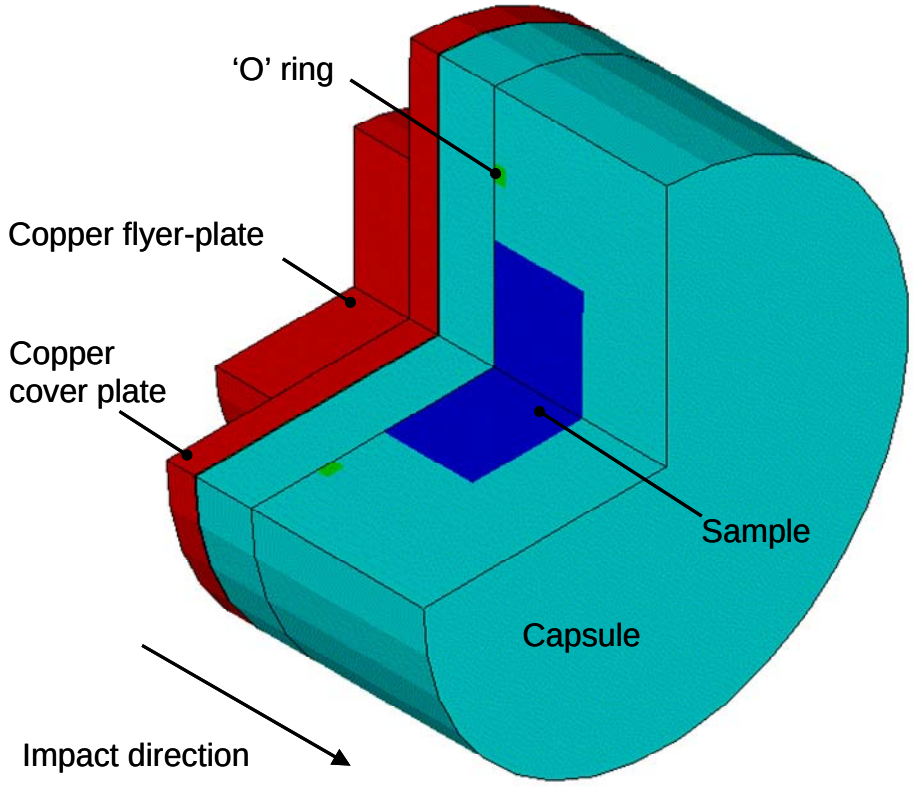

Figure 2: Numerical set-up in ANSYS® AUTODYN (no air gap); the flyer plate is seen to the rear of the image.

RESULTS AND DISCUSSION

Stress history in the AISI 304 L

Below are the results recorded from experiments conducted with an impact velocity of 345 m/s and 446 m/s. These results are compared with data from the simulations where a gauge point is encapsulated in 500 μm of epoxy resin (two cell widths).

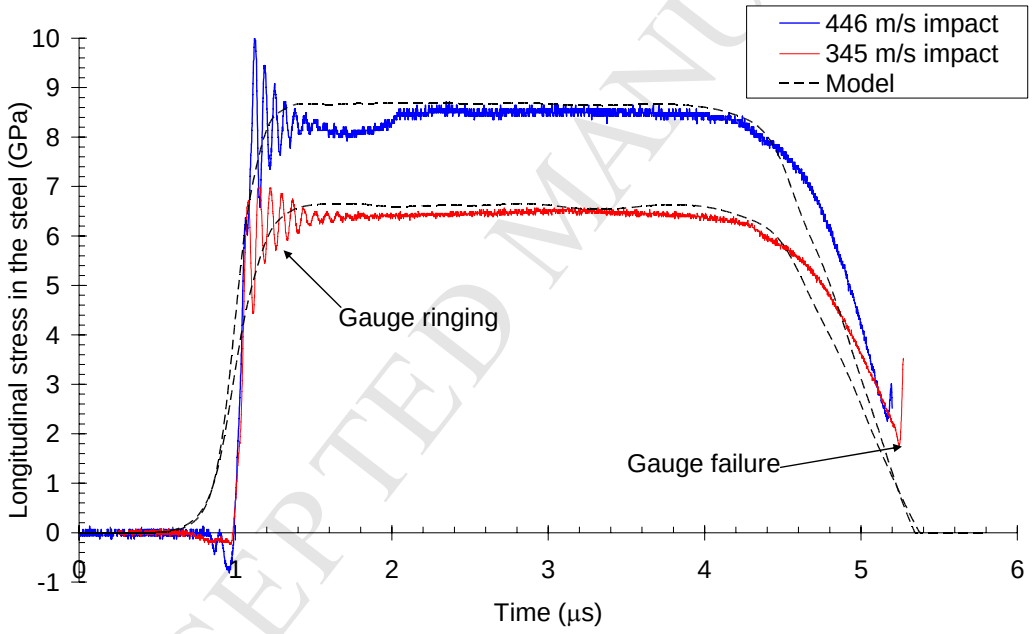

Figure 3: Shock stress seen in the AISI 304 L steel during the experiments; the simulation results are provided for comparison.

There are several things to note from Figure 3. Firstly, it can be seen from both experiments that the shock is characterised by a very fast rise time (c. 100 ns) resulting in ringing in the gauge. This ringing is electrical in nature and is commonly

reported for these types of gauges embedded between metallic plates [31]. Secondly, it should be pointed out that the rise time observed in the models was relatively slow compared to experiments. This is to be expected and is due to the shock wave being smeared across the cells. The gauge is seen to fail in both experiments at roughly the same time and is probably due to the extensive plastic deformation observed in the copper cover plate coupled with the arrival of the release wave.

Pressure history in the fluid layer

From 1D hydrodynamic calculations using the Rankine-Hugoniot relationships, the magnitude of the shock in the fluid layer was calculated as initially being 0.64 GPa and 0.87 GPa for the experiments with an impact velocity of 345 m/s and 446 m/s respectively. However, 2D simulations using ANSYS® AUTODYN showed that the shock was higher than this in the fluid layer due to ringing. Figure 4 shows the pressure history in a capsule that has been struck by a copper flyer plate at 446 m/s. At 0 μs (a reference time corresponding to 8 μs after impact), a shock of magnitude 0.8 GPa is seen to propagate in the fluid layer. Eventually this shock wave reaches the fluid / steel boundary; 5 μs later it is seen to have been reflected. The reflection resulted in a pressure increase as the shock wave travels back towards the impact interface. Eventually, the shock wave encounters the stainless steel cover plate that is deforming due to it being pressed into the cavity. Consequently, on contact with the stainless steel cover plate, the shock in the fluid layer undergoes a shape change from a reasonably flat wave to that of a divergent wave. In essence, the shock wave rang up in the fluid layer before dissipating to a steady state.

The suppression of the cavitation that would have otherwise occurred was due to the thickness of the flyer plate and by virtue of the deformation of the cover plate attached to the main cup of the capsule assembly. Figure 5 shows the deformation of the cover from the experiment and the simulation; in both cases the impact velocity of the flyer plate was 446 m/s. Firstly it can be seen that the distinct similarity of the final profile gives confidence in the Johnson-Cook model for the stainless steel that was taken from [26]. Secondly, it is evident that the ductility of the steel used here was advantageous in allowing the plastic flow into the cavity. Consequently, the choice of a ductile steel that is able to flow, over and above a relatively strong steel that would have provided little ductility is desirable.

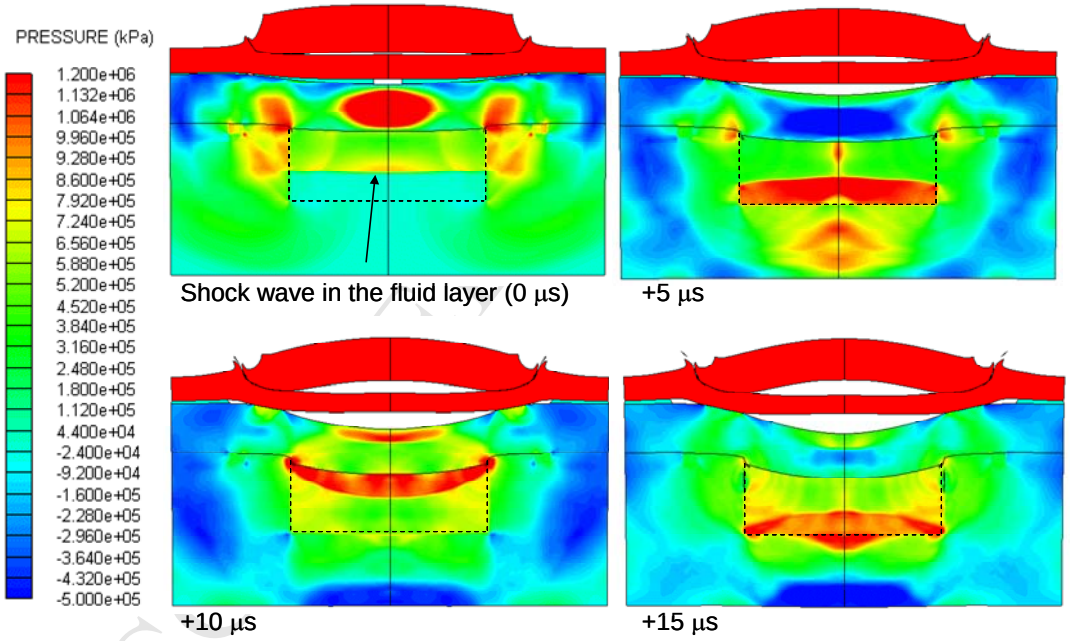

Figure 4: ANSYS® AUTODYN simulation of the experiment without the air cavity; velocity of impact = 446 m/s.

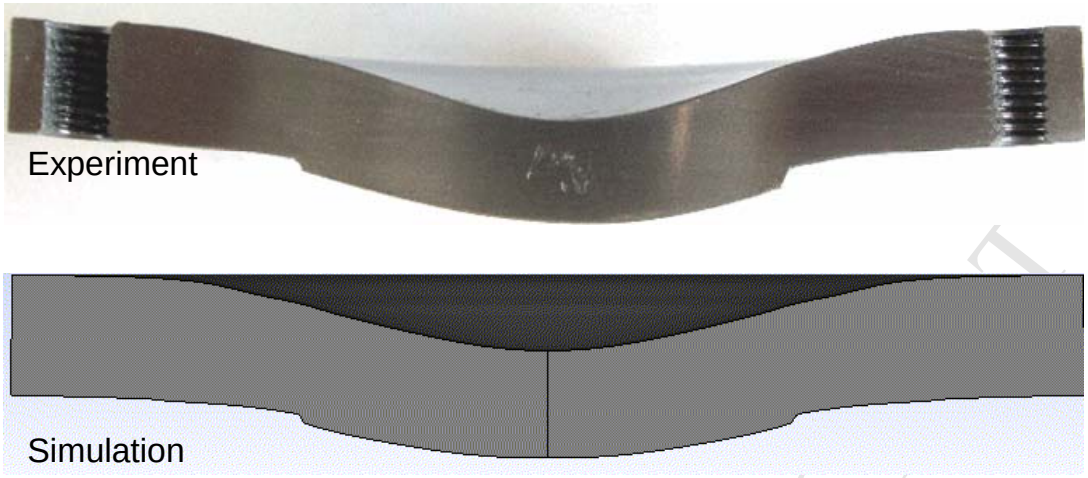

Figure 5: Deformation of the cover plate showing the results from an impact at 446 m/s for both the experiment (top) and the simulation (bottom).

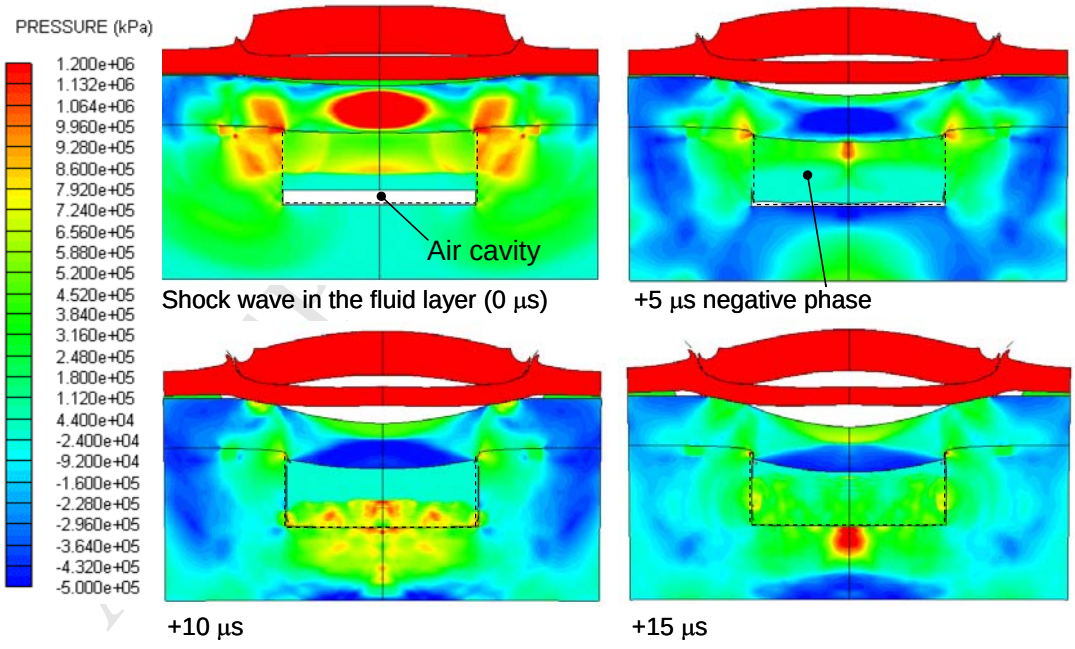

Figure 6: ANSYS® AUTODYN simulation of the experiment with the air cavity; velocity of impact = 446 m/s.

Introducing a cavity behind the fluid layer resulted in a different response as shown in Figure 6. The simulation has been done using the same impact velocity as the case presented in Figure 4 for comparison. Again, the shock is seen to traverse the fluid layer however 5 μs later, due to the presence of the cavity, a negative pressure phase occurs as the release wave propagates from the membrane barrier towards the direction of the impact face. This resulted in a condition where the fluid layer is essentially "stretched" [32]. A second shock occurs as the fluid contacts the base of the cavity and propagates back towards the impact face. Eventually, the shock again rings up within the fluid layer before reaching a steady state. By 15 μs, erosion of the lagrangian cells within the encapsulated fluid is evident.

The loading regime for these experiments is considerably different to the first set of experiments and consequently subjected the fluid to a negative pressure thereby invoking cavitation followed by reloading.

The numerical calculations of the pressure history in the suspension for both types of experiments (velocity of impact = 446 m/s) are presented in Figures 7 and 8. In each case, the pressure history over 40 μs is presented for two gauge tracer points located in a line at 10.00 mm from the axis of symmetry and placed at 0.25 mm and 10.25 mm from the interface between the stainless steel cover plate and the suspension.

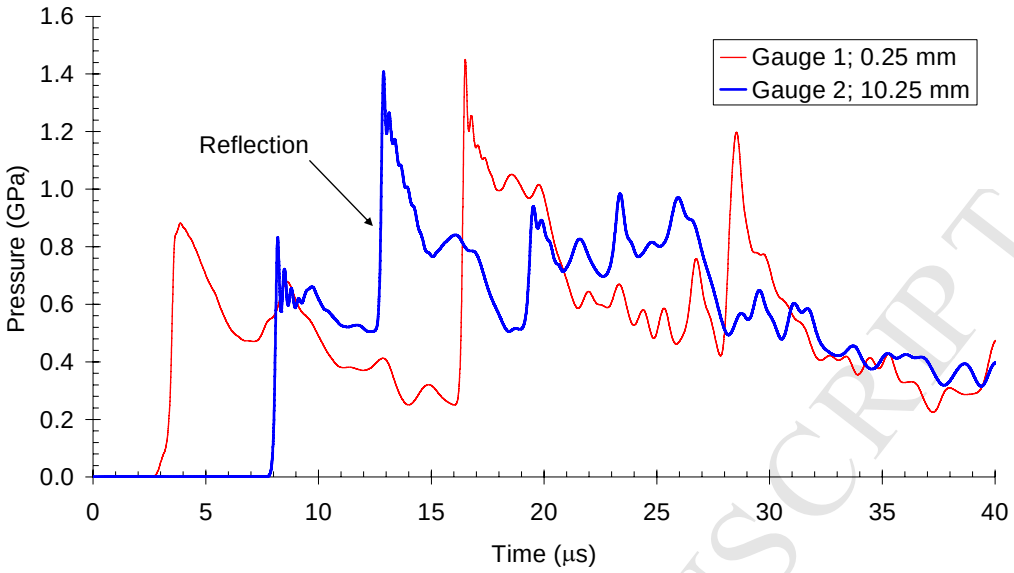

Figure 7: Pressure history calculations from the simulation without the air cavity; velocity of impact = 446 m/s.

For the pressure-history trace of the experiment without the air gap (Figure 7), the initial shock in the suspension is seen at 3 μs from the point of time of impact by the copper flyer-plate. The shock state is seen to release at this gauge location before reload occurs at c.a. 16 μs due to the reflection of the shock wave from the stainless steel rear boundary. At Gauge-point 2, the reload is seen to occur much quicker by virtue of the fact that this gauge location is closer to the rear boundary than Gauge 1. Finally, the pressure dissipated to a steady state of c.a. 0.2 GPa at 100 μs (not shown).

Where the air cavity was introduced, the pressure history is shown in Figure 8.

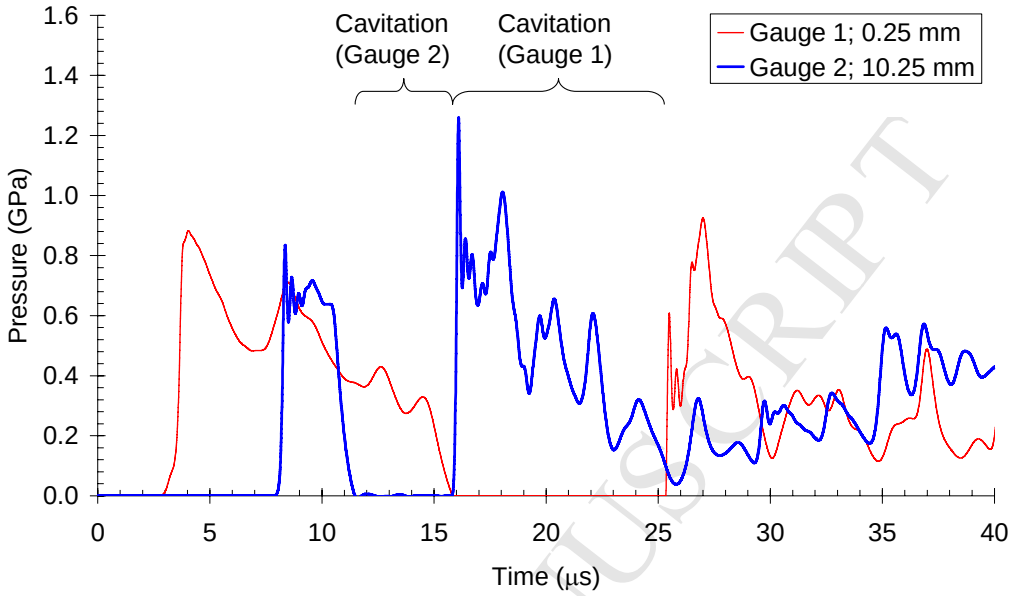

Figure 8: Pressure history calculations from the simulation with the air cavity; velocity of impact = 446 m/s.

Again the arrival of the pressure pulse is seen to occur at c.a. 3 μs before releasing to P= 0 GPa at c.a. 16 μs. The second gauge shows the release of the shock at c.a. 11 μs before a rapid reload at 16 μs. The second reload was caused by the impact of the suspension against the rear stainless steel surface (see Figure 6).

Effect of the compression on the fluid layers

Analysis of the shocked specimens showed that the compression pulse had little effect on the bacterial samples when cavitation was suppressed; no reduction in numbers was observed when compared to the control (unshocked) specimen. This is somewhat surprising given the high compression that was achieved using this technique and given that other researchers have noted bacterial kill with much lower

pressures [7,8]. This confirms that the mechanisms of kill were not dependent on the *magnitude* of the pressure but rather the degree of repetition and, perhaps, exposure to UV light. It should be pointed out that the materials in the structure of the cells do have very similar shock properties to the medium in which they are suspended. Nevertheless, it is known that the cell walls of microorganisms such as *Saccharomyces cerevisiae* [33] do possess small but finite stiffness values. Consequently, it is envisaged that very high single shock pressures are required to cause delamination of the cell structure. Willis et al. [13] did see mortality in their specimens that were shocked in a fluid medium to higher shock states observed here. One suggested explanation the observed mortality was put down to the shock–induced phase transformation during near-isentropic compression of the suspension leading to the formation of ice VI or ice VII. These high pressure phases are 20 % to 25 % denser than the liquid and consequently would lead to over pressures in the liquid cytoplasm. An alternative explanation was also provided by Willis et al. for the observed cell mortality. The density variations in the cell's makeup may give rise to Richtmyer-Meshkov fluid instabilities induced by the shock acceleration of the interfaces between each cell layer. However, this latter explanation appears less likely given the shock pressures achieved in our experiments and the observed survivability.

However, when the air-gap was introduced in the cavity limited kill was observed with 1-log reduction in the yeast sample only. Given the violence associated with cavitation, it is perhaps surprising that these microorganisms demonstrate significant survivability. These results confirm the hardy nature of micro-organisms that have been subjected to shock loading as noted by Burchell et al. [6, 12].

Perhaps more enlightening are the effects that the shock wave had on the emulsification of the oil-based solutions. Figure 9 shows the effect on the sample

when the sample has been subjected to shock compression and where cavitation had been suppressed (with no air gap). The coarse emulsions prior to the passage of the shock wave possessed a volume mean particle size of 13.6 μm with a distribution (by % volume) of particle sizes as follows: 10% ≤ 1.2 μm, 50% ≤ 13.0 μm and 90% ≤ 25.1 μm. After the passage of the shockwave, the droplet size distribution changed, producing smaller droplets with a volume mean particle size of 8.2 μm and a distribution of: 10% ≤ 1.2μm, 50% ≤ 7.3 μm and 90% ≤ 16.7μm.

For the second experimental setup where cavitation was expected, significant emulsification occurred as shown in Figure 10. After the passage of the shockwave, the droplet size distribution changed, producing smaller droplets with a volume mean particle size of 7.8 μm and a distribution as follows: 10% ≤ 0.7 μm, 50% ≤ 2.6 μm and 90% ≤ 16.5 μm. These results demonstrate a shift in population from 10-20 micrometres to 1-10 micrometres (see Figure 11) that remained stable when tested 7 days later. We should point out however that this occurred at a higher impact velocity (441 m/s as opposed to 345 m/s). Nevertheless, it is probable that the increased impact velocity should have little effect on the degree of cavitation as this is solely governed by wave reflections. To the authors' knowledge, no work has been done to examine high pressure shock wave interaction with emulsions, although ultrasonic approaches have been extensively studied [34-37]. Current thinking suggest that emulsification by ultrasound at least is governed by a localised cavitation zone [38]. These results are consistent with our shock studies and confirm that the capsule is behaving as expected from the modelling results. However, as noted above, a certain degree of emulsification has occurred in Figure 9. Consequently, as we are suppressing cavitation in this experimental setup, a different mechanism of break up must be at play and this demands explanation. One possibility is that the divergent wave front

reflected from the deforming cover plate (see Figure 4) is inducing shear in the oil droplets. This may well be expected to cause a breakdown of the particle however we are unable to verify this using the current setup.

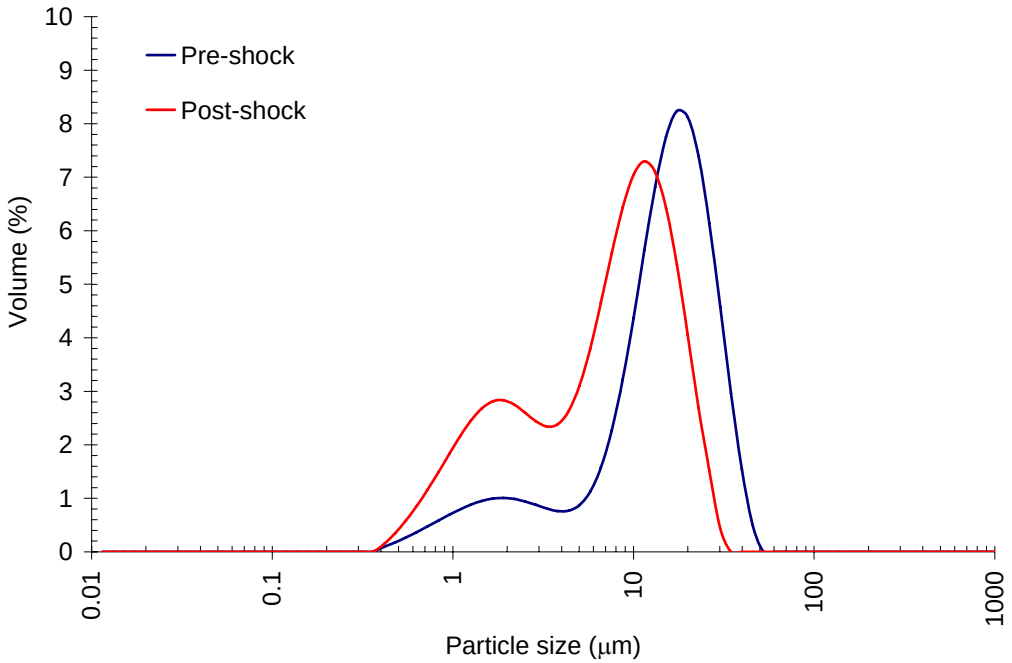

Figure 9: Pre and post shock particle distribution (no air gap at the rear); velocity of impact = 345 m/s.

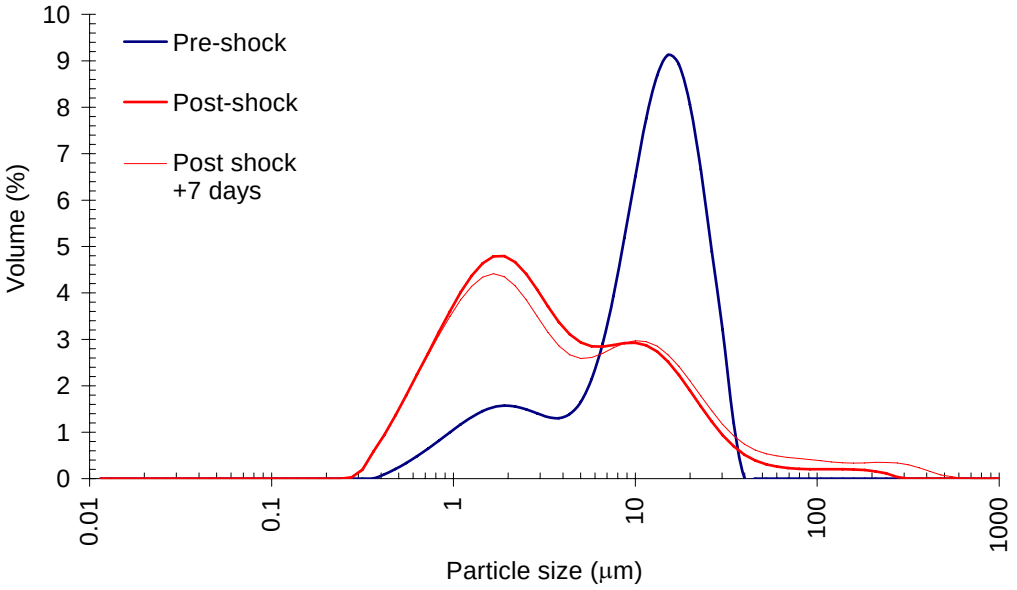

Figure 10: Pre and post shock particle distribution (with an air gap at the rear); velocity of impact = 441 m/s.

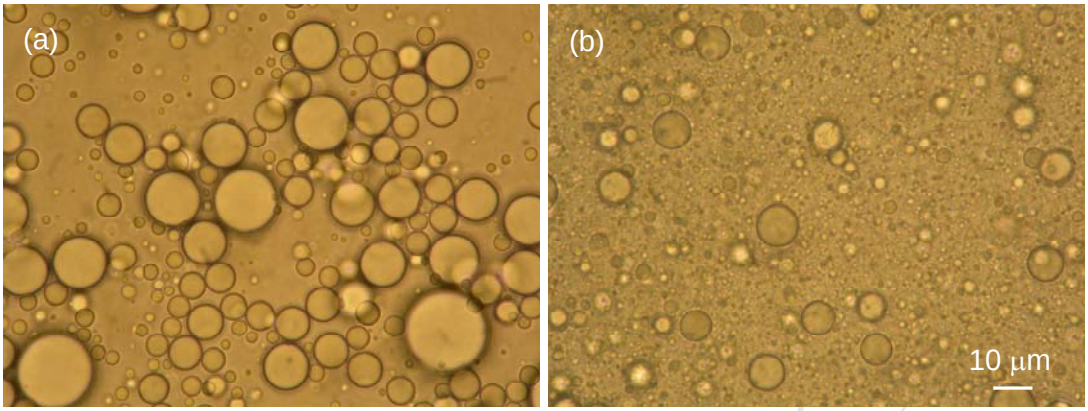

Figure 11: Light micrographs of (a) Emulsion before treatment and (b) emulsion after the passage of the shock wave (with air gap).

CONCLUSIONS

Different bacterial solutions have been subjected to shock loading where the magnitude of the shock wave in the suspension approached c.a. 1.2 GPa. It was found that using a ductile cover plate for the capsule resulted in suppression of cavitation in the fluid layer by virtue of extrusion of the plate into the cavity. The capsules were recovered intact so that post experimental analysis could be done on the contents. Furthermore, we have also shown that microorganisms such as *Zygosaccharomyces bailii*, *Escherichia coli* and *Enterococcus faecalis* are not affected by this type of loading regime. However, a limited amount of emulsification of a simple oil water mixture did occur and it was thought that this was most likely due to the presence of the divergent wave front due to the deforming front plate.

By introducing a cavity behind the fluid sample it was possible to encourage cavitation and consequently, increase the degree of emulsification that occurred. This resulted in the formation of a stable emulsion. It was also noted that the yeast sample

suffered a 1-log reduction in numbers due to the passage of the shock wave and resulting violence from cavitation; the bacterial sample was largely unaffected. Further, other researchers have noted significant bacterial kill with much lower pressures [1,7,8]. This confirms that the mechanisms of kill in the earlier work were not purely dependent on the *magnitude* of the pressure but rather the degree of repetition and, perhaps, exposure to UV light.

Numerical simulations of the experiments were conduced using ANSYS® AUTODYN that showed good correlation with the experimental results.

ACKNOWLEDGEMENT

We would like to thank Mr Gary Cooper for helping with the design of the capsule and supporting the experiments. We also would like to thank Mr Chris Stennett for useful discussions. This work was funded under the LINK collaborative research programme (project AFM 264). The funding by DEFRA (UK) is gratefully acknowledged as are the contributions by Arla Foods UK plc., Britvic plc., and RTS (Leeds). Finally, we gratefully acknowledge the support of ANSYS® AUTODYN.

REFERENCES

1. Loske A M, Alvarez, U M, Hernandez-Galicia C, Castano-Tosado E, Prieto F E. Bacterial effect of underwater shock waves on Escerichia coli ATCC 10536 suspension. Innovative Food Science and Emerging Technologies 2002;3: 321-327.

2. Williams-Campbell AM, Solomon MB, Reduction of spoilage microorganisms in fresh beef using hydrodynamic pressure processing. Journal of Food Protection 2002; 65 (3): 571-574.
3. Podolak R, Solomon MB, Patel JR, Liu MN, Effect of hydrodynamic pressure processing on the survival of Escherichia coli O157:H7 in ground beef. Innovative Food Science & Emerging Technologies 2006; 7 (1-2): 28-31.
4. Stöffler D, Horneck G, Ott S , Hornemann U, Cockell CS, Moeller R, Meyer C, de Vera J, Fritz J, Artemieva NA. Experimental evidence for the potential impact ejection of viable microorganisms from Mars and Mars-like planets. Icarus 2007; 186: 585–588.
5. Teshima K, Ohshima T, Tanaka S, Nagai T. Biomechanical effects of shock waves on Escherichia coli and λphage DNA. Shock Waves 1995; 4: 293-297.
6. Burchell MK, Mann J, Bunch AW, Brandão BFP, Survivability of Bacteria in Hypervelocity Impact, Icarus 2001;154:545-547.
7. Loske AM, Prieto FE, Zavala ML, Santana AD, Armenta E. Repeated application of shock waves as a possible method for food preservation. Shock Waves 1999; 9: 49-55.
8. Zuckerman H, Krasik Y E, Felsteiner J. Inactivation of microorganisms using pulsed high underwater discharges. Innovative Food Science and Emerging Technologies 2002; 3: 329-336.
9. Abe A, Mimura H, Ishida H, Yoshida K. The effect of shock pressures on the inactivation of a marine Vibrio sp. Shock Waves 2007; 17: 143-151.
10. Alvarez A, Ramirez A, Fernandez F, Mendez A, Loske M. The influence of single-pulse and tandem shock waves on bacteria. Shock Waves 2008; 17: 441-447.

11. Kani K, Biological effects of shock pressure on microorganism. Materials Science Forums 2004; 465-466: 117-122.
12. Burchell MJ, Mann JR, Bunch AW. Survival of bacteria and spores under extreme shock pressures. Mon. Not. R. Astron. Soc. 2004; 352: 1273–1278.
13. Willis MJ, Ahrens TJ, Bertani LE, Nash CZ. Bugbuster—survivability of living bacteria upon shock compression. Earth and Planetary Science Letters 2006; 247: 185–196.
14. Whiteman G, Millett J C F, Bourne N K. Longitudinal and lateral stress measurements in Stainless steel 304L under 1D shock loading. In Shock Compression of Condensed Matter - 2007, edited by M. Elert, M. D. Furnish, R. Chau, N. Holmes, and J. Nguyen. 2007 American Institute of Physics pp. 673-676.
15. McQueen R G, Marsh S P, Taylor J W, Fritz J N, Carter W J. High-Velocity Impact Phenomena (1970).
16. Bass JD, Ahrens TJ, Abelson JR, Hua TJ, Shock temperature measurements in metals: New Results for an Fe Alloy. Geo. Res. 1990; 95: 21767-21776.
17. Gallagher K G, Bass J D, Ahrens T J, Fitzner M, Abelson JR, Shock-temperature of stainless steel and a high pressure-high temperature constraints on thermal diffusivity of AL2O3. High-Pressure Science and Technology - 1993, ed. S.C. Schmidt et al, Amer. Inst. Phys., New York, p. 963-966 (1994).
18. Rosenberg Z, Yaziv D Partom Y. Calibration of foil-like manganin gauges in planar shock wave experiments. J. Appl. Phys 1980; 51: 3702-3705.
19. Bourne NK, A 50 mm bore gas gun for dynamic loading of materials and structures. Meas Sci Technol 2003; 14: 273-278.

20. Robertson N, Hayhurst C, Fairlie G, Numerical simulation of impact and fast transient phenomena using AUTODYN(TM)-2D and 3D. Nuclear Engineering and Design 1994; 150:235-241.

21. Anderson, Jr. CE, An overview of the theory of hydrocodes. Int J of Impact Engng 1987; 5:33-59.

22. Meyer MA, Dynamic behaviour of materials. New York: John Wiley & Sons; 1994.

23. Johnson GR, Cook WH, Fracture characteristics of three metals subjected to various strains, strain rates, temperatures and pressures. Eng Fract Mech 1985;21: 31-48.

24. Anderson CE Jr, Sharron TR, Walker JD, Freitas CJ, Simulation and analysis of a 23-mm HEI projectile hydrodynamic ram experiment. Int J Impact Engng 1999; 22: 981-997.

25. Nagayama K, Mori Y, Shimada K, Shock Hugoniot compression curve for water up to 1 GPa by using a compressed gas gun. J Appl Phys 2002; 91 (1): 476-482.

26. Xue Q, Nesterenko VF, Meyers MA. Evaluation of the collapsing thick-walled cylinder technique for shear-band spacing. Int J Impact Engng 2003; 28 (3): 257-280.

27. Eakins DE, Thadhani NN. Instrumented Taylor anvil-on-rod impact tests for validating applicability of standard strength models to transient deformation states. J of Appl Phys 2006; 100: 073503.

28. Bourne N K, Millett JCF, The high-rate response of an elastomer. Proc R Soc Lond A 2003; 459: 567-576.

29. Hazell P J, Stennett C, Cooper G. The shock and release behaviour of an aerospace-grade cured aromatic amine epoxy resin. Polym Compos 2008; 29:1106-1110.

30. Boteler JM, Sutherland GT. Tensile failure of water due to shock wave interactions. J Appl Phys 2004; 96 (11): 6919-6924.

31. Bourne NK, Rosenberg Z. On the ringing observed in shock-loaded piezoresistive stress gauges. Meas Sci Technol 1997; 8: 570–573.

32. Caupin F, Herbert E. Cavitation in water: a review. C. R. Physique 2006 ;7 :1000–1017.

33. Smith AE, Zhang Z, Thomas CR, Moxham KE, Middelberg APJ. The mechanical properties of Saccharomyces cerevisiae. PNAS 2000; 97 (18): 9871–9874.

34. Abismaïl B, Canselier J P, Wilhelm A M, Delmas H, Gourdon C. Emulsification by ultrasound: drop size distribution and stability. Ultrasonics Sonochemistry 1999; 6: 75–83.

35. Li M K, Fogler H S. Acoustic emulsification. Part 2: Breakup of the large primary oil droplets in a water medium. Journal of Fluid Mechanics 1978; 88: 513–528.

36. Wood W, Loomis A L. The physical and biological effects of high-frequency sound waves of great intensity, Philosophical Magazine and Journal of Science 1927; 44: 417–436.

37. Jafari S M, He Y, Bhandari B. Production of sub-micron emulsions by ultrasound and microfluidization techniques, Journal of Food Engineering 2007; 82:478–488.

38. Cucheval A Chow R C Y. A study on the emulsification of oil by power ultrasound. Ultrasonics Sonochemistry 2008; 15: 916-920.

LIST OF CAPTIONS

Figure 1: An exploded view of the capsule design; all dimensions are in mm.

Figure 2: Numerical set-up in ANSYS® AUTODYN (no air gap); the flyer plate is seen to the rear of the image.

Figure 3: Shock stress seen in the AISI 304 L steel during the experiments; the simulation results are provided for comparison.

Figure 4: ANSYS® AUTODYN simulation of the experiment without the air cavity; velocity of impact = 446 m/s.

Figure 5: Deformation of the cover plate showing the results from an impact at 446 m/s for both the experiment (top) and the simulation (bottom).

Figure 6: ANSYS ®AUTODYN simulation of the experiment with the air cavity; velocity of impact = 446 m/s.

Figure 7: Pressure history calculations from the simulation without the air cavity; velocity of impact = 446 m/s.

Figure 8: Pressure history calculations from the simulation with the air cavity; velocity of impact = 446 m/s.

Figure 9: Pre and post shock particle distribution (no air gap at the rear); velocity of impact = 345 m/s.

Figure 10: Pre and post shock particle distribution (with an air gap at the rear); velocity of impact = 441 m/s.

Figure 11: Light micrographs of (a) Emulsion before treatment and (b) emulsion after the passage of the shock wave (with air gap).

TABLES

Table 1: Elastic properties of the AISI 304 L material used to manufacture the capsule.

Material	ρ_0 (g/cc)	c_L (mm/μs)	c_S (mm/μs)	G (GPa)	ν
AISI 304L	7.903	5.739	3.155	78.5	0.283

Table 2: Summary of flyer-plate experiments. In each case a 10-mm copper flyer-plate was used.

Sample	Flyer velocity (m/s)	Air-gap?
Bacteria	345	No
Yeast	446	No
Emulsion	345	No
Bacteria	448	Yes
Yeast	450	Yes
Emulsion	441	Yes

Table 3: Hydrodynamic data for the copper, stainless steel, water and the epoxy resin.

	Notation	Copper	AISI 304L	H_2O	Epoxy resin
Reference density (kg/m^3)	ρ_0	8,900	7,903	1,000	1,186
Bulk sound speed (m/s)	c_0	3,958	4,570	1,483	2,730
Slope in U_s versus U_p diagram	S	1.497	1.49	1.75	1.493
Grüneisen coefficient	Γ	2.00	1.93	0.28	1.13

Table 4: Strength data for the copper and stainless steel; the Johnson-Cook data for the stainless steel was taken from [26]; the data for the copper was provided by [27].

	Notation	Copper	AISI 304L
Yield strength (MPa)	A	90	110
Work hardening constant (MPa)	B	292	1500
Work hardening exponent	n	0.05	0.36
Strain rate hardening coefficient	C	0.005	0.014
Melting temperature (°K)	T_m	1356	1696
Reference temperature (°K)	T_{room}	300	300
Thermal softening coefficient	m	1.09	1.0